ELSEVIER

Journal of Alloys and Compounds 320 (2001) 296–301

Journal of ALLOYS AND COMPOUNDS

www.elsevier.com/locate/jallcom

Selection of promising quaternary candidates from Mg–Mn–(Sc, Gd, Y, Zr) for development of creep-resistant magnesium alloys ☆

J. Gröbner, R. Schmid-Fetzer*

Technical University of Clausthal, Institute of Metallurgy, Robert-Koch-Str. 42, D-38678 Clausthal-Zellerfeld, Germany

Abstract

Recently developed Mg–Mn–Sc alloys show a considerable increase of creep resistance at elevated temperature. The endeavor to further improve the properties and to reduce cost of high-price Sc metal initiated a search for additional alloying elements. Gd, Y and Zr were considered for this purpose. The aim is to achieve a large quantity of suitable precipitations to improve mechanical properties using a minimum of expensive alloy element addition. The huge amount of possibilities of combining the elements Mg–Mn–(Sc, Gd, Y, Zr) and the time and cost effort of technological experiments require a preselecting of systems and alloy compositions. Thermodynamic phase diagram and phase amount calculations were performed to give hints for selecting promising candidates. A priority list of three quaternary systems is established: Mg–Mn–Gd–Sc, Mg–Mn–Sc–Y and Mg–Mn–Y–Zr, based on the classification of individual alloys. Most promising is MgMn1Gd5Sc0.8 (wt.%), but the alloys MgMn1Gd5Sc0.3 and MgMn1Y5Sc0.8 are also promising. The entire quaternary Mg–Mn–Y–Zr system is disqualified because of phase diagram features that are detrimental for the required microstructural engineering. The focused alloy development following this approach avoids a waste of time and effort.

Keywords: Phase diagrams; Alloy development; Thermodynamic calculation; Magnesium; Manganese; Scandium

1. Introduction

Recently developed Mg–Mn–Sc alloys show considerably increasing creep resistance at elevated temperature [1]. Initially, investigations started with binary Mg–Sc alloys. Scandium was chosen for hardening by ageing because of its large solubility in Mg and the retrograde solubility at lower temperatures. In fact, the Mg–Sc phase diagram [2] shows a peritectic, which is a rare exception among the binary Mg systems. However, MgSc precipitates were formed very slowly during ageing and improved the mechanical properties only slightly because of their incoherent interface. Therefore, Mn was added as a second alloying element. Mn_2Sc precipitations form coherently and were found useful for improving creep resistance, hardness and strength of Mg alloys. New MgSc15Mn1 or MgSc6Mn1 alloys show about 100 times better creep-resistance than best commercial WE43 alloy at 350°C and 30 MPa [1].

The endeavor to further improve the properties and to reduce cost of high-price Sc metal initiated a search for additional alloying elements. Gd, Y and Zr were considered for this purpose. The aim is to achieve a large quantity of suitable precipitations to improve mechanical properties using a minimum of expensive alloy element addition. Gadolinium and yttrium were considered since they form stable Mg-rich binary compounds which might be precipitated during ageing at low temperatures in larger amounts. Zirconium was considered as a potential complete replacement for scandium.

At this point the problem is, that the element combinations Mg–Mn–(Sc, Gd, Y, Zr) form a variety of quaternary systems and within those there is a huge amount of possibilities to select alloy compositions. The time and cost effort of technological experiments involving large volume melting and casting, sample preparation and mechanical testing, requires a preselection of alloy systems and alloy compositions.

Phase diagram calculations were performed to give hints for selecting promising candidates. Here we report on

☆This study was presented at Calphad XXVIII, Grenoble, France, 2–7 May 1999. Dedicated in honoring memory of Alan Prince.

*Corresponding author.

E-mail address: schmid-fetzer@tu-clausthal.de (R. Schmid-Fetzer).

0925-8388/01/$ – see front matter
PII: S0925-8388(00)01480-8

establishing a priority list of three quaternary systems: Mg–Mn–Gd–Sc, Mg–Mn–Sc–Y and Mg–Mn–Y–Zr, and also to indicate promising compositions within these systems. The basic idea is to use calculated phase diagrams as road maps to find shortcuts and to avoid costly detours during development of advanced Mg-alloys.

2. Thermodynamic data assessment

Reliable and mutually consistent thermodynamic data for the binary subsystems are the key prerequisites to perform any reasonable calculation in the higher order systems. Twelve binary systems are needed in the present case. The data sets of the binary edge systems Mg–Mn [3], Gd–Mg [4], Mg–Sc [2], Mn–Sc [5], Mg–Y [6], Mg–Zr [7], and Mn–Y, Mn–Zr, Y–Zr [8] were taken from the literature. Systems with missing data (Gd–Mn, Gd–Sc, and Sc–Y) were estimated by our own optimization which will be described in detail in separate publications.

Using these data sets, calculations can be performed by extrapolation into the 10 ternary subsystems involved in the three quaternary systems. Ternary phases are not known in these systems. Extrapolation means that the Gibbs energy functions of solution phases in the ternary (e.g. liquid) are constructed from the binary functions without ternary interaction parameters. These extrapolations have been checked in the following way. In five ternary systems, Mn–Y–Zr, Mg–Mn–Sc, Mg–Mn–Y, Mg–Mn–Zr and Mg–Y–Zr, experimental data are available and they are all in agreement with the calculated phase equilibria. The system Mn–Y–Zr was studied in detail [8]. For Mg–Mn–Sc a comparison is published [1], for the other ternaries it will be published separately. Calculated diagrams of the remaining six ternary systems Mg–Mn–Gd, Mg–Gd–Sc, Mn–Gd–Sc, Mg–Y–Sc, Mn–Y–Sc and Mn–Y–Zr have been carefully studied and plausibility checks were performed.

Based on this assessment of the data sets for the binary and ternary subsystems, phase equilibria of the quaternary systems Mg–Mn–Gd–Sc, Mg–Mn–Y–Sc and Mg–Mn–Y–Zr can be calculated by extrapolation. It is reasonable to assume that quaternary compounds do not exist. General experience shows that the number of compounds drastically decreases from binary to ternary systems and that quaternary compounds are virtually unknown. Similarly, quaternary solution phases originating from the binary or ternary edge systems are usually reasonably well described by construction from the binary and ternary thermodynamic functions. This is especially true for the solution phases in one of the corners of the composition tetrahedron, like the (Mg) solid solution in the Mg-rich corner. Even though actual quaternary experimental data could be used to check or even improve the thermodynamic data sets, it is the predictive and extrapolation capability that makes computational thermochemistry such a powerful tool for multicomponent alloys. The additional information needed decreases drastically when proceeding from binary to ternary or even higher order systems.

3. Relating phase diagrams and alloy processing

Alloy compositions were studied in the ranges of 0–1.5 wt.% Mn, 0–10 wt.% Sc, Zr and 0–10 wt.% RE (RE=Gd, Y). The calculated quaternary phase equilibria are presented in two-dimensional sections and most useful are T–x sections (or vertical sections, isopleths) in the Mg-rich corner with just one composition variable, x, over the entire temperature range, T, relevant for melting, solidification and heat treatment. Most of the sections were calculated with constant Mn and RE content as T–x(Sc) sections, since one aim was to minimize the Sc content of promising alloys. For fixed alloy composition the thermodynamic basis enables the additional calculation of property diagrams, showing the phase amounts or phase compositions over a temperature range.

How to identify promising alloy candidates from all these calculated diagrams? What is needed is a ‘wish list’ of beneficial phase diagram features, derived from the relevant alloy processing steps. The important topics on such a list are highlighted in Table 1.

A simple and cheap melting process requires liquidus temperatures well below 800°C. During solidification the

Table 1
Beneficial phase equilibrium features and their relevance for (Mg)-alloy processing

Phase diagram feature	Relevance for alloy processing
Liquidus temperature $\ll 800$°C	Melting process simple and cheap
Primary phase field L+(Mg)	Primary solidification of (Mg) matrix, avoid primary growing precipitates
Primary (Mg) phase amount high at end of L+(Mg) phase field	Ensure sufficient growth of (Mg) matrix during primary solidification
(Mg) single-phase field	Enables homogenization annealing
Solid state (Mg)+precipitate(s) field	Enables microstructural engineering
Precipitate amount=proper $f(T)$: Sufficient amount below T_{max} (~550°C) and above T_{min} (~ 300°C)	T_{max} low enough to avoid big precipitates, T_{min} high enough for good kinetics and thermal stability

primary growth of precipitates should be avoided. Such precipitates, growing freely into the melt, tend to be large and detrimental. In other words, the (Mg) matrix should be the primary phase to grow and this requires a primary L+(Mg) phase field. Also the amount of the primarily grown (Mg) matrix should be sufficiently large at the end of this L+(Mg) field, before the first precipitates appear. This can be seen from phase amount diagrams for a specific alloy. The direct visualization from the *T–x* phase diagram in the quaternary is usually impossible, in contrast to binary *T–x* diagrams, where the lever rule could be applied.

Heat treatment aiming at homogenization of the common segregation after solidification requires the existence of a (Mg) single phase field in the phase diagram. It should be not too narrow to permit a robust technical homogenization. The existence of solid state two-phase or multi-phase fields (Mg)+precipitate(s) is essential for microstructural engineering, for example by precipitation hardening or, if homogenization is unfeasible, by ageing. The amounts of precipitates must also be sufficiently large and moreover formed in an appropriate temperature regime between T_{max} and T_{min} of about 550°C to 300°C. The upper limit, T_{max}, should be low enough to avoid the growth of big precipitates during cooling. The lower limit, T_{min}, should be high enough to provide good kinetic growth conditions and also to ensure thermal stability of the final material for application at elevated temperature.

All these criteria have been checked by calculation and analysis of phase and property diagrams to determine promising alloys, which in addition must comply with the condition of low cost alloying elements. At the end, a priority list of quaternary systems was established and promising alloy compositions indicated. This is discussed in the following, showing only a small fraction of the calculated diagrams as examples.

4. Mg–Mn–Gd–Sc alloys

The exemplary *T–x* section with constant Mn (1 wt.%) and Gd (5 wt.%) from the Mg-corner to 1 wt.% Sc (Fig. 1) shows favorable liquidus temperatures around 650°C and a wide range of primary crystallization of (Mg) up to 0.85 wt.% Sc. Various vertical sections from 0 to 10 wt.% Sc with constant Gd content of 5, 8, 10 and 12 wt.% and 1 wt.% Mn were calculated. A comparison of the different sections shows that increasing Gd content diminishes the one-phase field of (Mg). This homogeneity range of (Mg) becomes smaller because both the solidus line is shifted downwards and the Sc-solubility is shifted to lower values with increasing Gd content. To achieve a large (Mg) one-phase field, a small content of Gd is desirable. However, 5 wt.% Gd seems a reasonable compromise, since at lower values the phase amounts of precipitating

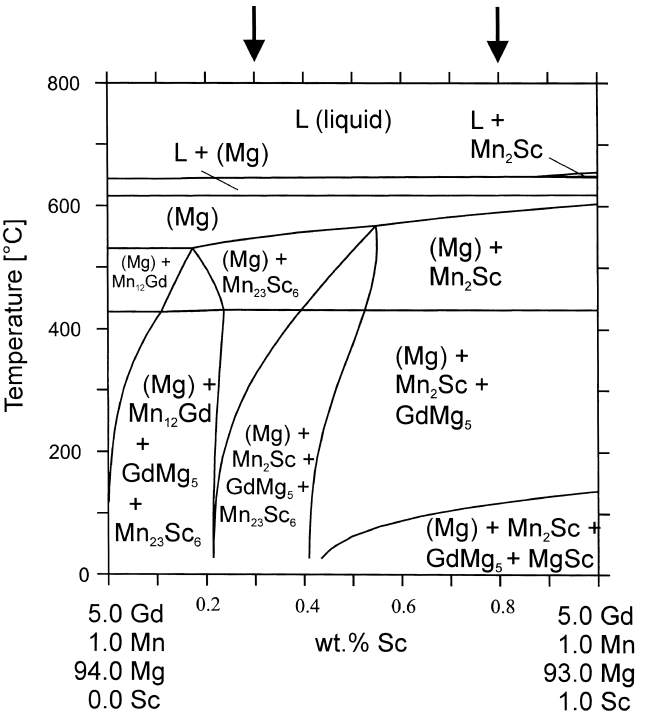

Fig. 1. Mg–Mn–Gd–Sc phase diagram section at constant 1 wt.% Mn and 5 wt.% Gd. Arrows indicate two alloys examined in Figs. 2 and 3.

Gd-compounds become too low, as seen from separate calculations.

For a fixed alloy composition of 0.8 wt.% Sc (MgMn1Gd5Sc0.8) the sequence of phase equilibria during cooling is L+(Mg), (Mg), (Mg)+Mn_2Sc, (Mg)+Mn_2Sc+$GdMg_5$, and (Mg)+Mn_2Sc+$GdMg_5$+MgSc. This qualitative information from Fig. 1 is presented with quantitative phase amounts in Fig. 2. It is most easily read starting in the upper right corner with 1 mol liquid at the liquidus point, 650°C, that is consumed at the solidus point, 619°C, while the primary (Mg) matrix grows from 0 to 1 mol. The inset in Fig. 1, scaled up to 0.1 mol, clearly shows that, below the narrow single-phase (Mg) range, the first solid-state precipitate Mn_2Sc starts forming at 590°C and its growth is almost completed around 400°C. The second precipitate, $GdMg_5$ starts at 425°C, and reaches 80% of its final amount already at 300°C. The final precipitate MgSc is not important, not only because of the low starting temperature of 110°C but also because it is known from the binary Mg–Sc system that it forms very slowly and has an insignificant influence on mechanical properties. Summarizing the message of Fig. 2 in comparison with Table 1, the alloy MgMn1Gd5Sc0.8 is very promising. Melting and solidification behavior is feasible, and especially the precipitates Mn_2Sc and $GdMg_5$ form in an ideal temperature range in reasonable or even large amounts.

The next step is to check if these promising properties could be retained for a smaller amount of expensive scandium addition of only 0.3 wt.% Sc. Fig. 3 shows the

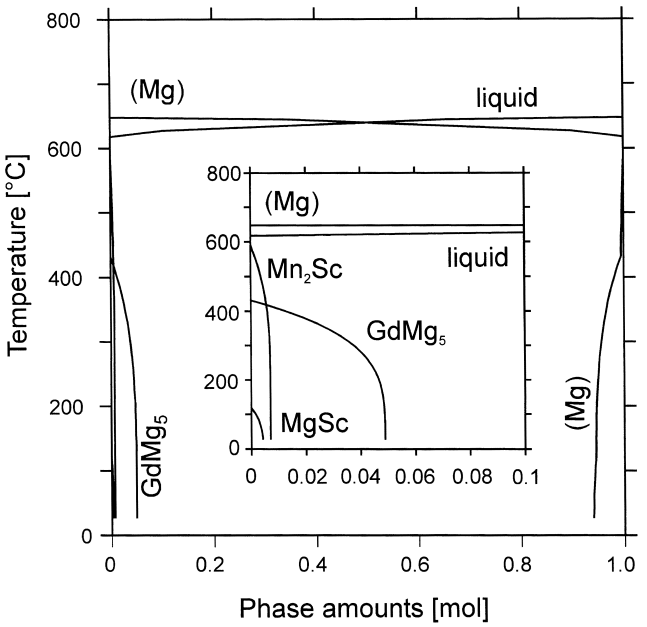

Fig. 2. Equilibrium phase amounts of the alloy MgMn1Gd5Sc0.8 (wt.%). All phase amounts are given in moles, referring to mol of atoms, throughout this study.

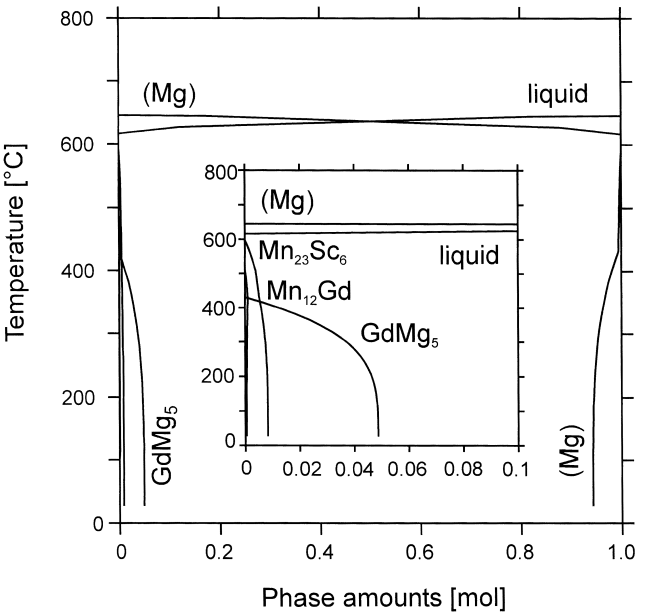

Fig. 4. Equilibrium phase amounts of the alloy MgMn1.5Gd5Sc0.3 (wt.%).

calculated results for this MgMn1Gd5Sc0.3 alloy. Primary solidification is virtually unchanged. However, the single-phase field of (Mg) is extended to lower temperature, also seen in Fig. 1. The first precipitate forming is now the Mn-richer $Mn_{23}Sc_6$ compound whereas Mn_2Sc only forms below 310°C and in smaller amounts. It shares the scandium with $Mn_{23}Sc_6$. Some scandium is of course dissolved in (Mg). The formation profile of $GdMg_5$ is almost exactly identical for both alloys, comparing Fig. 3 and Fig. 2. In summary, the MgMn1Gd5Sc0.3 alloy is also promising. Positive is the small Sc-content and the wider (Mg) field. Unknown is the efficiency of $Mn_{23}Sc_6$ for improving the alloy properties.

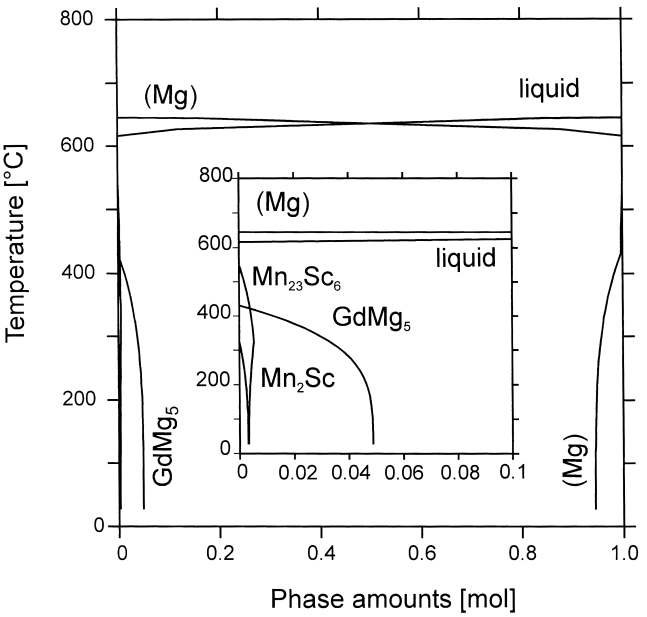

Fig. 3. Equilibrium phase amounts of the alloy MgMn1Gd5Sc0.3 (wt.%).

Since the manganese–scandium precipitates are of interest, it was checked if a higher manganese content might help to exploit the expensive scandium dissolved in (Mg) even better. The result is shown in Fig. 4 for the alloy MgMn1.5Gd5Sc0.3 with 1.5 wt.% Mn. Now $Mn_{23}Sc_6$ starts forming at about 50°C higher temperature, narrowing the single-phase (Mg) field. No Mn_2Sc is formed at all, but a new precipitate, $Mn_{12}Gd$. It is plausible that the more Mn-rich compounds will form at higher Mn-content and the calculation shows that actually 1 wt.% Mn is a reasonable limit. The alloy MgMn1.5Gd5Sc0.3 is a questionable one, especially because of the complete absence of Mn_2Sc, which has already demonstrated its efficiency in improving the creep-resistance [1]. It has still to be tested if $Mn_{23}Sc_6$, $Mn_{12}Gd$ or $GdMg_5$ are effective precipitates.

5. Mg–Mn–Y–Sc alloys

Yttrium and gadolinium are considered as alternative alloying elements. Here the effect of replacing Gd by Y in the quaternary Mg–Mn–Y–Sc system is studied. Fig. 5 shows an exemplary *T–x* section with constant Mn (1 wt.%) and Y (5 wt.%) from the Mg-corner to 1 wt.% Sc. Liquidus and solidus lines are very similar to Fig. 1. The (Mg) single-phase region, however, is much narrower, excluding a robust technical homogenization treatment. Ageing may be an option though, because of the interesting ranges of various precipitates forming at, say, 0.8 wt.% Sc. For an alloy MgMn1Y5Sc0.8 the corresponding phase

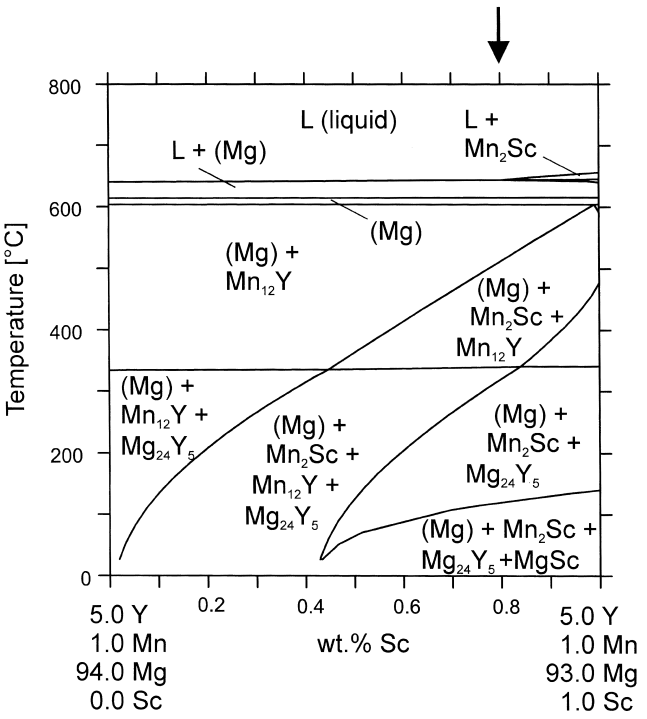

Fig. 5. Mg–Mn–Y–Sc phase diagram section at constant 1 wt.% Mn and 5 wt.% Y. Arrow indicates the alloy examined in Fig. 6.

amounts are given in Fig. 6. The $Mn_{12}Y$ phase would only be stable in the solid state in a high temperature range from 605 to 322°C and may not form at all during fast cooling. The established Mn_2Sc and the new $Mg_{24}Y_5$, even in very large amount, could form by ageing in a favorable temperature range. This makes MgMn1Y5Sc0.8 also a promising alloy.

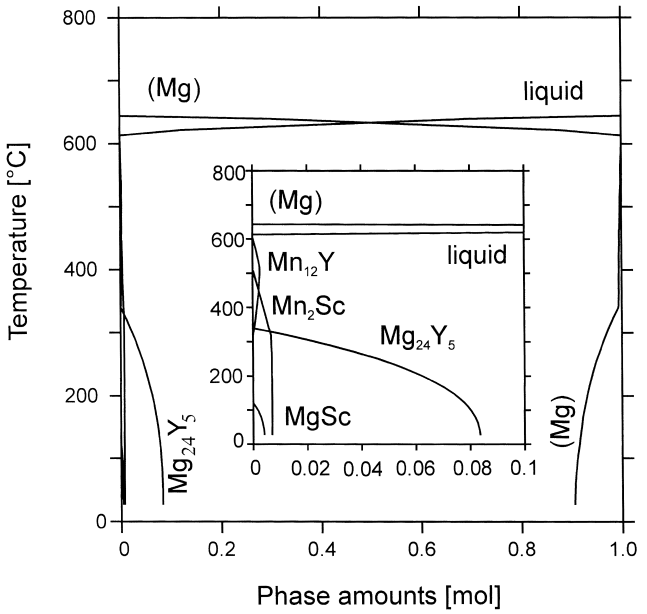

Fig. 6. Equilibrium phase amounts of the alloy MgMn1Y5Sc0.8 (wt.%).

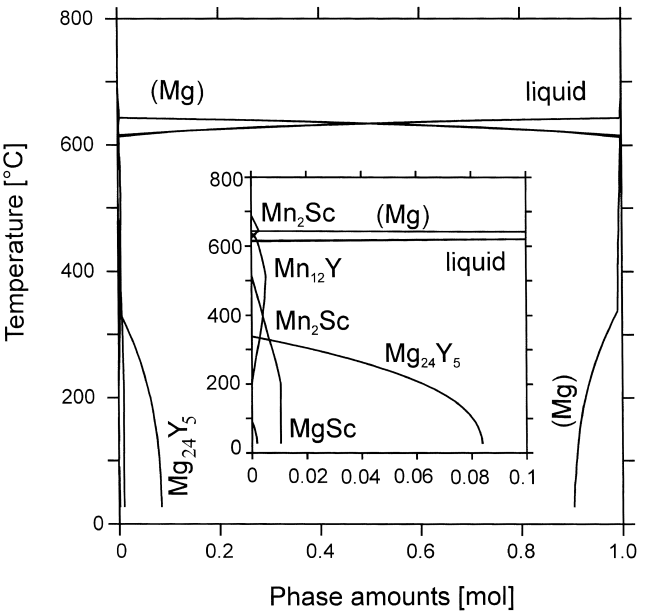

Fig. 7. Equilibrium phase amounts of the alloy MgMn1.5Y5Sc0.8 (wt.%).

In order to check if the amount of Mn_2Sc could be raised by increasing the manganese content to 1.5 wt.%, we can examine Fig. 7 for the alloy MgMn1.5Y5Sc0.8. This alloy is disqualified since Mn_2Sc forms as the primary phase from the liquid, clearly seen in the inset of Fig. 7. (Mg) forms only secondary, and even $Mn_{12}Y$ forms as a tertiary phase during solidification. Such a microstructure cannot be 'repaired' by annealing.

6. Mg–Mn–Y–Zr alloys

Zirconium can be considered as a possible alloying element for complete substitution of expensive scandium. The impact of such a substitution can be studied in Fig. 8 for scandium-free alloys with 1 wt.% Mn, 4.5 wt.% Y and 0–1 wt.% Zr. This phase diagram section shows a very steeply rising liquidus line, 1000°C are reached for less than 0.1 wt.% Zr. Moreover, and actually the reason for the steep liquidus line, a huge primary crystallization field, $L+Mn_2Zr$, stretches over the entire composition range in Fig. 8. Only for extremely small Zr-additions, not discernible in Fig. 8, is a primary (Mg) solidification expected. The reason for this destructive phase diagram feature is the extremely high thermodynamic stability of Mn_2Zr in comparison to the other phases. Since yttrium does not play a significant role in that part, the only way to diminish the $L+Mn_2Zr$ primary field would be a drastic reduction of the manganese content. But this would also drastically reduce the amount of beneficial Mn-containing precipitates. As a result, the entire quaternary Mg–Mn–Y–Zr alloy system is disqualified.

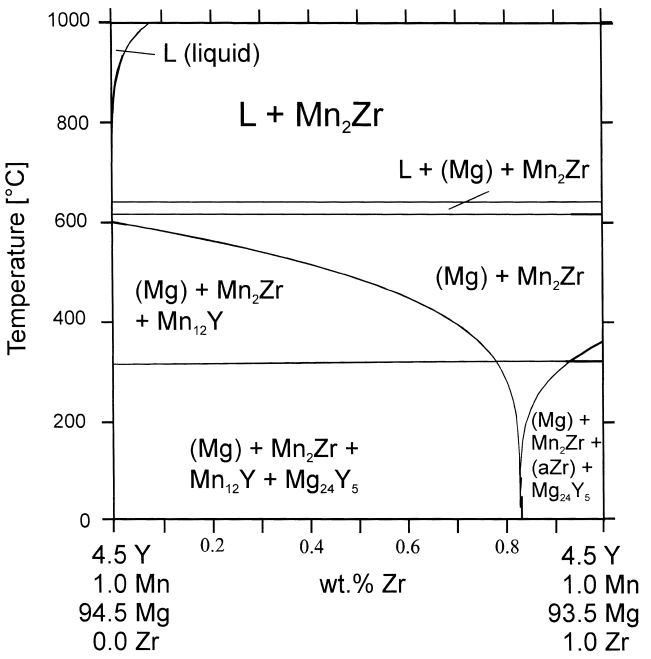

Fig. 8. Mg–Mn–Y–Zr phase diagram section at constant 1 wt.% Mn and 4.5 wt.% Y.

7. Conclusion

Alloy compositions with promising possibilities of alloy microstructure design could be selected by means of thermodynamically calculated phase diagrams and phase amount charts. Element combinations and compositions with unwanted properties could be recognized before starting large-style experiments, thus reducing the experimental effort to a reasonable volume.

The following priority list of quaternary systems and individual alloy compositions for the development of creep-resistant Mg-alloys is found:

1. Mg–Mn–Gd–Sc system. Alloy MgMn1Gd5Sc0.8 is very promising, alloy MgMn1Gd5Sc0.3 is promising and alloy MgMn1.5Gd5Sc0.3 is questionable.
2. Mg–Mn–Y–Sc system. Alloy MgMn1Y5Sc0.8 is promising, alloy MgMn1.5Y5Sc0.8 is disqualified.
3. Mg–Mn–Y–Zr system. Entire quaternary system is disqualified.

The next step, the experimental study of mechanical properties of alloys from that list is currently under way. Obviously, these experiments cannot be replaced by thermodynamic calculations. However, considering the huge number of less promising alloy combinations that could be selected from Mg–Mn–(Sc, Gd, Y, Zr), the focused alloy development following this approach avoids a waste of time and effort.

Acknowledgements

This work is supported in the ‘Thrust Research Project SFB 390: Magnesium Technology’ by the German Research Council (DFG).

References

[1] F.v. Buch, B.L. Mordike, A. Pisch, R. Schmid-Fetzer, Development of Mg–Mn–Sc alloys, Mater. Sci. Eng. A 263 (1999) 1–7.
[2] A. Pisch, R. Schmid-Fetzer, G. Cacciamani, P. Riani, A. Saccone, R. Ferro, Mg-rich phase equilibria and thermodynamic assessment of the Mg–Sc system, Z. Metallkd. 89 (1998) 474–477.
[3] J. Tibballs, System Mg–Mn, in: I. Ansara, A.T. Dinsdale, M.H. Rand (Eds.), COST507 — Thermochemical Database for Light Metal Alloys, European Commission, 1998, pp. 215–216, EUR 18499 EN.
[4] G. Cacciamani, Private communication, 1998.
[5] A. Pisch, R. Schmid-Fetzer, Experimental study and thermodynamic assessment of phase equilibria in the Mn–Sc system, Z. Metallkd. 89 (1998) 700–703.
[6] H.L. Lukas, System Mg–Y, in: I. Ansara, A.T. Dinsdale, M.H. Rand (Eds.), COST507 — Thermochemical Database for Light Metal Alloys, European Commission, 1998, pp. 224–226, EUR 18499 EN.
[7] M. Hämäläinen, System Mg–Zr, in: I. Ansara, A.T. Dinsdale, M.H. Rand (Eds.), COST507 — Thermochemical Database for Light Metal Alloys, European Commission, 1998, pp. 234–235, EUR 18499 EN.
[8] H. Flandorfer, J. Gröbner, A. Stamou, N. Hassiotis, A. Saccone, P. Rogl, R. Wouters, H. Seifert, D. Maccio, R. Ferro, G. Haidemenopoulos, L. Delay, G. Effenberg, Z. Metallkd. 88 (1997) 529–538.